Energy and Buildings 101 (2015) 95–109

Contents lists available at ScienceDirect

Energy and Buildings

journal homepage: www.elsevier.com/locate/enbuild

Net-zero and beyond! Design and performance of NIST's net-zero energy residential test facility

A. Hunter Fanney[a,b,*], Vance Payne[a,b], Tania Ullah[a,b], Lisa Ng[a,b], Matthew Boyd[a,b], Farhad Omar[a,b], Mark Davis[a,b], Harrison Skye[a,b], Brian Dougherty[a,b], Brian Polidoro[a,b], William Healy[a,b], Joshua Kneifel[a,b], Betsy Pettit[a,b]

[a] Engineering Laboratory, National Institute of Standards and Technology, Gaithersburg, MD 20899 USA
[b] Building Science Corporation, 30 Forest Street, Somerville, MA 02143, USA

ARTICLE INFO

Article history:
Received 14 October 2014
Received in revised form 23 April 2015
Accepted 3 May 2015
Available online 11 May 2015

Keywords:
Net-zero energy buildings
Photovoltaic
Solar thermal
Air-to-air heat pump
Heat recovery ventilator
Test facility
National Institute of Standards and Technology

ABSTRACT

A Net-Zero Energy Residential Test Facility has been constructed at the National Institute of Standards and Technology to demonstrate that a home similar in size, aesthetics, and amenities to those in the surrounding communities can achieve net-zero while meeting the needs of a four member family. The home incorporates a vast array of renewable energy and energy efficient technologies, a subset of which was used during the first year of operation, including an air-to-air heat pump system, a solar photovoltaic system, a solar thermal hot water system, and a heat recovery ventilation system (HRV). The solar photovoltaic system generated 13,523 kW h of energy, exceeding the home's annual energy consumption by 484 kW h during the 12-month test interval. The solar thermal hot water system provided 54% of the energy required to meet the hot water load. Use of the heat recovery ventilator, used to provide ventilation air to the home, resulted in 1965 kW h of energy consumption, 514 kW h to power the HRV and 1451 of energy used by the heat pump system to meet the additional sensible and thermal loads. This paper describes the facility and presents performance data for the first year of operation.

Published by Elsevier B.V.

1. Introduction

Buildings consumed 41% of all energy used in the United States in 2010, with residential buildings and commercial buildings accounting for 22 and 19% [1], respectively. In addition to consuming more energy than the transportation or industrial sector, buildings represent the fastest growing sector of energy usage [1]. In order to address the significant amount of energy consumed by residential buildings, a number of net-zero energy houses have been designed, constructed and monitored throughout the world. Parker [2] presents a history of low energy residential homes and presents annual performance data from a dozen very low energy homes in North America. Parker concludes that very low energy homes can be readily achieved in the U.S., and the greatest cost effectiveness is achieved through energy efficiency measures as opposed to the use of renewables. Musall et al. [3] summarizes the research of the International Energy Agency's Annex 52 "Towards Net Zero Energy Buildings" and states that "during the last 20 years more than 200 reputable projects with the claim of a net-zero energy budget have been realized all over the world." Musall reiterated the finding of Parker that efficiency measures need to be implemented before consideration of renewable energy sources and further notes that less on-site energy generation offers a greater number of architectural options. Rosta et al. [4] report on the construction and performance of a zero-energy house in the Desert Southwest region of the U.S. Boleyn [5] reports on a residence in Portland, Oregon that is approaching net-zero in a relatively cloudy climate. Doiron, O'Brien, and Athienitis [6] present design, construction and detailed performance data for a residence located near Montreal. They document the large influence of occupant behavior on energy consumption. Sherwin et al. [7] present the performance of four near net-zero energy homes in Florida instrumented to provide data on electrical consumption and generation, indoor conditions, and meteorological conditions. Norton et al. [8]

* Corresponding author at: National Institute of Standards and Technology, Engineering Laboratory, Gaithersburg, MD 20899, USA. Tel.: +1 3019755864.
E-mail addresses: hunter.fanney@nist.gov (A.H. Fanney), vance.pane@nist.gov (V. Payne), tania.ullah@nist.gov (T. Ullah), lisa.ng@nist.gov (L. Ng), matthew.boyd@nist.gov (M. Boyd), farhad.omar@nist.gov (F. Omar), mark.davis@nist.gov (M. Davis), harrison.skye@nist.gov (H. Skye), brian.dougherty@nist.gov (B. Dougherty), brian.polidoro@nist.gov (B. Polidoro), william.healy@nist.gov (W. Healy), joshua.kneifel@nist.gov (J. Kneifel), betsy@buildingscience.com (B. Pettit).

http://dx.doi.org/10.1016/j.enbuild.2015.05.002
0378-7788/Published by Elsevier B.V.

Fig. 1. Net-zero energy residential test facility (NZERTF).

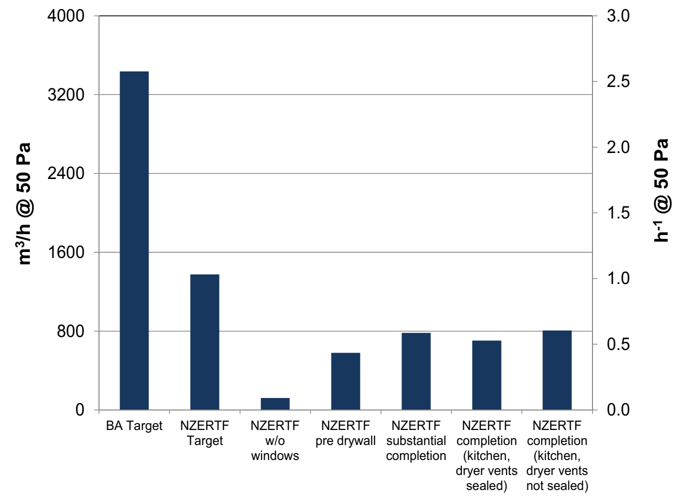

Fig. 2. blower door test results at various stages of construction.

report on the design and performance of a 118.9 m^2, three-bedroom Habitat for Humanity zero energy home near Denver, Colorado that produced 24% more energy than it consumed during its first year of operation.

In 2012 NIST completed the construction of a Net-Zero Energy Residential Test Facility (NZERTF) on its campus in Gaithersburg, MD to demonstrate that it was possible to achieve net-zero for a house with conventional architecture, amenities, and size comparable to those being constructed in the surrounding area. The living area of the NZERTF (252 m^2) is slightly larger than average size home (242 m^2) currently being constructed in the United States. Additionally the NZERTF is providing experimental data for computer model validation studies and to quantify the energy impact of mechanical ventilation. The purpose of this manuscript is to describe the design of the facility, to present data collected during the first year of operation, and to discuss a number of lessons learned. The cost-effectiveness of the various means used to achieve net-zero, comparisons of the actual versus modelled performance of the NZERTF, and benchmarking to other net-zero energy buildings will be addressed in future publications.

2. Design

The NZERTF is a unique facility in that it resembles a residence yet is truly a laboratory, Fig. 1. Among the NZERTF's unique features is access to three separate ground source heat exchangers, a radiant basement floor heating system, a solar hot water system with variable solar collector area and storage capacity, a 10.2 kW photovoltaic system, a heat recovery ventilation system, and various means of interfacing the smart grid with smart appliances. The facility also incorporates three different means of distributing conditioned air throughout the house—a sealed sheet-metal air distribution system; a high-velocity air distribution system; and provisions to incorporate a mini-split heat pump system. The NZERTF uses a smart meter to measure the energy imported and exported to the electric grid.

The house faces true south and is comprised of two stories (252 m^2) of living area and a full conditioned basement (135 m^2). The first floor includes the kitchen and dining area, a family room, an office (optional bedroom), a full bathroom, an open foyer to the second floor, and a utility closet. The second floor consists of a master bedroom with adjoining bathroom, two additional bedrooms, a second bath, and a hallway. The finished basement contains the vast majority of the facility's mechanical/electrical equipment whereas the detached garage contains the data acquisition/control equipment associated with the facility.

2.1. Building envelope

The building envelope was constructed using a continuous air barrier system to minimize infiltration with building ventilation provided by a heat recovery ventilation (HRV) system. Five blower door tests, Fig. 2, were conducted at various stages of construction, with the final test, conducted after the house was complete, yielding an air exchange rate of 802 m^3/h at 50 Pa corresponding to 0.63 air changes per hour. Building envelope components, Fig. 3, are described in the following sections. Detailed specifications, drawings, and construction can be found at the NZERTF webpage (http://www.nist.gov/el/nzertf/index.cfm).

2.1.1. Exterior above grade walls

The exterior above grade walls were constructed using nominal 5.1 cm × 15.2 cm wooden studs on 61 cm centers. The exterior sheathing is 1.3 cm-thick plywood. A continuous fully-adhered membrane that serves as an air and moisture barrier was applied to the plywood sheathing and sealed to the foundation wall. Exterior to the air and moisture membrane are two layers of 5.1 cm thick foil-faced polyisocyanurate foam board with the joints staggered and the outer layer sealed with tape. Wood furring strips, 2.5 cm × 10.1 cm, are secured to the structural framing elements using fasteners that pass through both layers of foam board into the framing elements. The exterior fiber cement lap siding is subsequently attached to the furring strips, resulting in a drainage plane behind the siding. The wall cavities are filled with blow-in cellulose insulation. The calculated *U*-factor [9] of the exterior above grade walls, including framing members, is 0.13 W/m^2-°C. The windows are double-hung units (rated *U*-factor of 1.14 W/m^2-°C) that incorporate a fully-insulated fiberglass frame, two panes of low-e coated glass with a suspended film positioned between the two panes of glass. The cavities between the panes of glass and the suspended film are filled with an inert gas.

2.1.2. Basement walls/floor

The basement walls were constructed of a 25.4 cm poured concrete wall with an integral 10.2 cm thick stem wall to accommodate the 35.6 cm deep open web floor joists. Damp proofing was applied to the exterior concrete walls. A 5.1 cm thick extruded polystyrene board was adhered to the interior of the concrete walls including the stem wall. A 5.1 cm thick foil-faced polyisocyanurate insulation board was applied over the extruded insulation with the exception of the stem wall area. Finally, 1.3 cm thick gypsum board was applied over the polyisocyanurate insulation. The

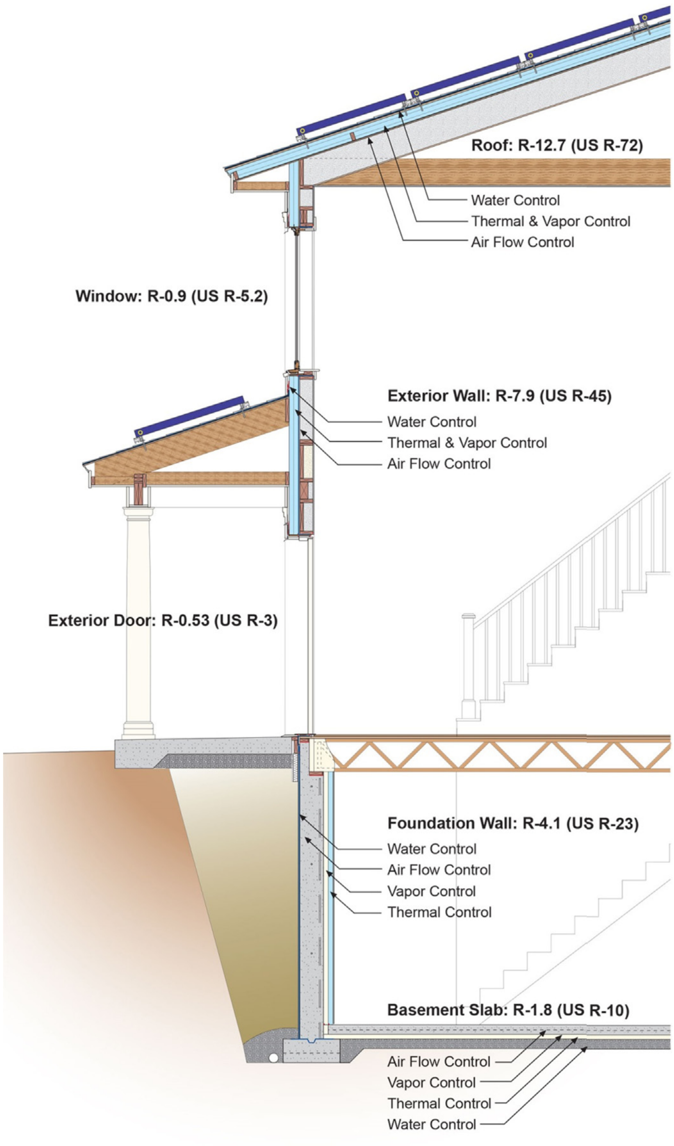

Fig. 3. Building envelope components and associated *R*-values.

calculated *U*-factor [9] of the basement exterior walls is 0.24 W/m^2-°C. Open cell spray foam insulation was used to fill the cavities between the floor joists where they rest on the stem wall. The concrete basement slab is 10.2 cm thick. Located beneath the concrete is a 0.15 mm polyethylene vapor barrier resting on 5.1 cm thick extruded polystyrene insulation. Embedded within the concrete slab is polyethylene tubing to be utilized for future radiant floor heating system research. The calculated *U*-factor [9] of the basement floor is 0.56 W/m^2-°C.

2.1.3. *Roof structure*

Unlike conventional residential construction, there is no insulation immediately above the second floor ceiling. The roof insulation is an integral part of the roof structure which consists of 1.3 cm thick plywood sheathing, a continuous fully-adhered air-moisture barrier, 12.7 cm of foil faced polyisocyanurate insulation applied in three layers (3.8 cm, 5.1 cm, and 3.8 cm), an additional 1.6 cm thick sheathing of plywood, a second fully-adhered air-moisture barrier, and finally asphalt shingles. The cavity between the 5.1 cm × 30.5 cm roof rafters, on 61 cm centers, was filled with blown-in cellulose insulation. The interior of the roof assembly was finished using 1.3 cm thick gypsum board. The calculated *U*-factor [9] of the roof structure, including framing elements, is 0.08 W/m^2-°C. Unlike conventional framing where the roof rafters are extended to provide the overhang, the overhangs are constructed using 5.1 cm × 10.2 cm framing applied over the air-moisture barrier, to reduce the thermal bridging effect of the overhangs. The header for the front porch that supports the porch roof rafters was also applied over the exterior wall insulation system to reduce thermal bridging.

3. Electrical, mechanical, and plumbing systems

3.1. *Electrical distribution system*

The NZERTF incorporates two separate electrical distribution systems. One distribution system, monitored by a smart meter, powers electrical loads typically found in a residence. The second electrical distribution system, not monitored by the smart meter, powers instrumentation and the devices used to simulate occupant sensible and latent heat loads. Each electrical circuit was carefully planned so that the electrical use of individual devices could be measured independently using instrumentation embedded in circuit breakers. Davis et al. [10] give a detailed overview of the overall monitoring architecture, sensors used, and the resulting measurement uncertainties associated with the electrical measurements. The electrical system incorporates a computer-controlled load control panel to switch on and off circuits throughout the house.

3.2. *Air-distribution systems*

The NZERTF has three independent duct systems: (1) an extensive duct system that can be utilized with air-to-air or ground source heat pumps referred to as the "large duct system"; (2) a small duct, high velocity (SDHV) air distribution system to be used in conjunction with an air-to-air SDHV heat pump (not used during the first year of operation); and (3) a dedicated duct system associated with the heat recovery ventilator (HRV). All ductwork is contained within the conditioned space. The large duct system, used during the first year of operation, was designed for less than 124.5 Pa pressure drop at supply and return duct airflow rates of 2039 m^3/h with all ducts fully open. The insulated main trunk lines are located with the indoor air handler in the basement. Multiple supply registers are located in each room of the house. Return ducts are located in central locations on the first and second floors. The duct system associated with the HRV, designed for a nominal airflow rate of 256 m^3/h, supplies ventilation air to all bedrooms and the kitchen, and exhausts air from all three bathrooms.

3.3. *Air-to-air heat pump system*

The heating and air conditioning system used for the first year of operation in the NZERTF consisted of an air source heat pump system that incorporates a dedicated dehumidification cycle, Fig. 4. The dedicated dehumidification cycle, available in the cooling mode only, is provided by control algorithms and a hot gas bypass arrangement with an additional indoor air heat exchanger that reheats the dehumidified air. The outdoor unit incorporates a two-speed scroll compressor with two modulated hot gas valves on the compressor discharge that send hot refrigerant gas through a third pipe to the reheat heat exchanger during active dehumidification. A supply air temperature sensor provides the control signal used to proportionally modulate the flow of hot refrigerant gas to maintain a preset supply temperature during dedicated dehumidification. The indoor air handler unit contains a variable speed indoor fan.

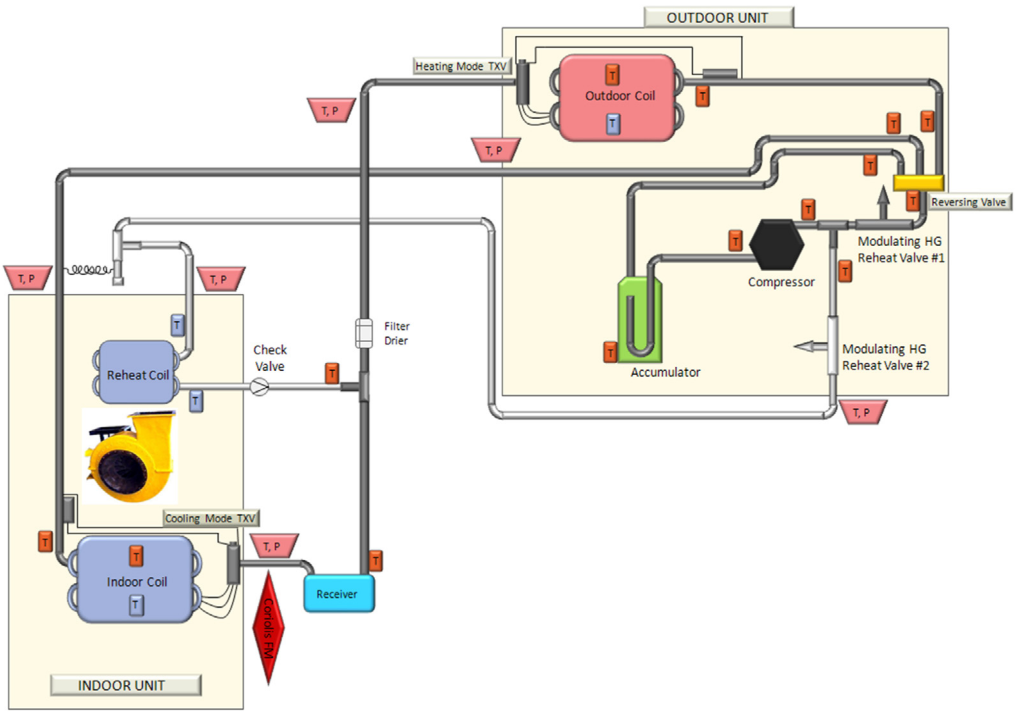

Fig. 4. heat pump refrigerant circuiting and instrumentation.

At the Air-Conditioning, Heating, and Refrigeration Institute (AHRI) rating conditions [11], the cooling capacity is 7.60 kW and the coefficient of performance (COP) is 3.82. In the heating mode at AHRI rating conditions, the unit has a heating capacity of 7.80 kW. The unit has a seasonal energy efficiency ratio (SEER—15.80 Btu/W h) of 4.63 W/W and a heating seasonal performance factor (HSPF Region IV—9.04 Btu/W h) of 2.65 W/W.

This single zone system has a thermostat located in the living room area of the first floor. During heating mode or defrost mode operations, the indoor unit controller may energize up to 10 kW of electric resistance heat. The thermostat set points in the cooling and heating modes are 23.8 °C and 21.1 °C, respectively. In the cooling mode, the thermostat is set such that the dehumidification mode of the heat pump unit is activated if the relative humidity reaches 50%. The instrumentation, data acquisition system, and measurement uncertainty associated with the heat pump system, as well as all other electrical/mechanical subsystems within the NZERTF are described in detail by Davis et al. [10].

3.4. Solar photovoltaic system

Thirty-two 320 W, positively-grounded photovoltaic modules with a nominal 19.6% efficiency are mounted on the main roof of the NZERTF at an 18.4° tilt, elevated approximately 14 cm above the asphalt shingle roof surface. Each module has 96 back-contact monocrystalline cells behind anti-reflective coated glass. The modules, each having an area of 1.63 m^2, are interconnected to form four parallel strings of eight series-connected modules. The power, voltage, and current at maximum power for the array at Standard Test Conditions (STC) [12] are 10.24 kW, 438 V, and 23.4 A, respectively. Meteorological instruments are located adjacent to the rooftop array and include an ambient temperature sensor in a passively vented, radiation shielded enclosure, an ultrasonic wind sensor located 0.6 m above the roof peak that measures the horizontal wind speed and direction, and a flat-plate monocrystalline silicon cell pyranometer that measures the irradiance in the plane of the array. Two 5 kW-rated inverters, having a measured weighted efficiency of 95.5% [13], are used to convert the direct current into 60 Hz alternating current (AC).

3.5. Solar hot water system

The residential test facility is equipped with two active, closed-loop solar water heating systems. During the first year of operation, only one of the two systems was used. The operational system utilizes two solar collectors and a 303 L storage tank with its 4500 W auxiliary heating element disabled, Fig. 5. The second system, which uses two separate solar collectors, utilizes a 454 L storage tank, will be used in future research in combination with the basement floor radiant heating system and/or ground source heat pump system. The solar collectors, heat exchangers, circulators, and controls are identical for both systems. Each solar thermal collector array consists of two SRCC OG-100 [14] certified single-glazed flat plate solar thermal collectors with individual aperture dimensions of 1.1 m by 2.0 m. The collectors are located on the porch roof, facing true south at an 18.4° tilt.

External to each solar storage tank is an insulated cross-flow heat exchanger, two circulating pumps, a controller, and two check valves to prevent reverse thermosyphoning when the pumps are not running. To prevent freezing, a 50% by volume propylene glycol in water solution is used in the solar thermal collector fluid loops. The controller turns the circulating pumps on when the temperature differential between these two sensors exceeds 10 °C and turns them off when the differential is below 3 °C. The controller de-energizes the circulators when the storage tank sensor exceeds 71 °C. The hot water leaving the solar storage tank enters a thermostatic mixing valve, set at 49 °C, before entering the downstream heat pump water heater. Temperature and flow measurements are made at multiple locations, as noted in Davis et al. [10].

3.6. Heat pump water heating system

Downstream of the solar hot water system, a heat pump water heater provides hot water in the event that the solar thermal water

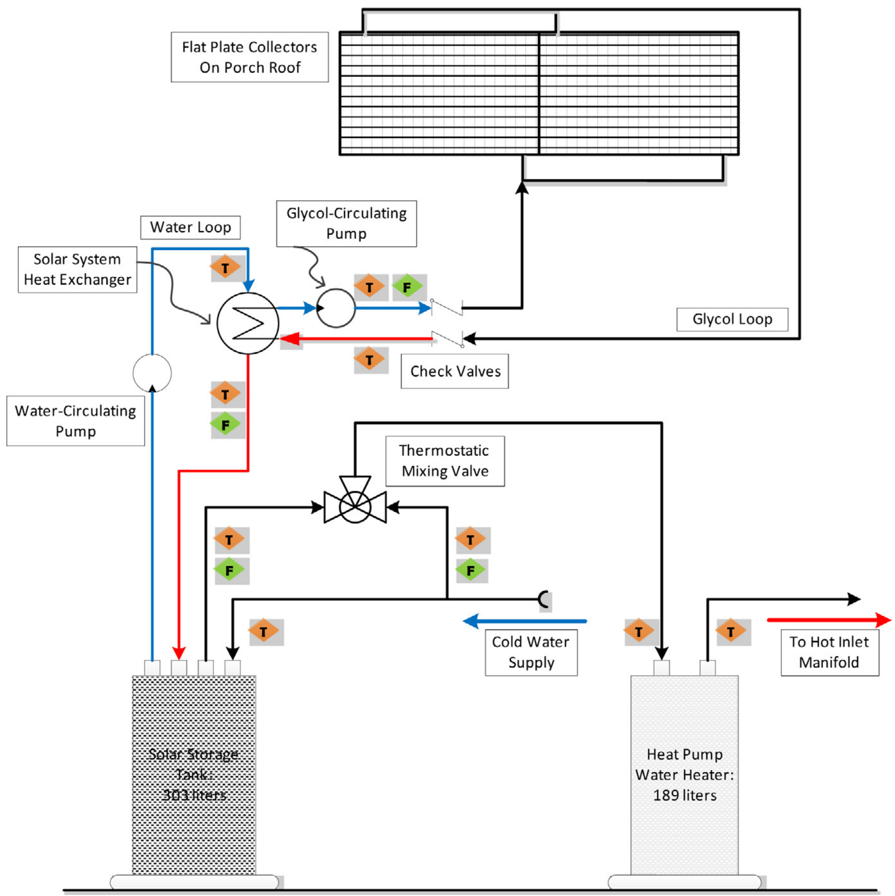

Fig. 5. Schematic of solar thermal and heat pump water heater.

heating system cannot meet the demand. The unit consists of a 189 L storage tank with an integrated heat pump water heater. The system is operated in the "Hybrid" mode with a temperature set-point of 49 °C. The "Hybrid" mode ensures that the heat pump provide a majority of the hot water load with a 3800 W resistive electric element being activated only in situations where the hot water demand cannot be met by the heat pump. In the "Hybrid" mode with a set-point temperature of 57 °C and an ambient temperature of 20 °C, the manufacturer-reported Energy Factor (EF), COP and standby loss of the unit are 2.5, 2.6, and 0.20 °C/h, respectively. In addition to monitoring the power consumption of the heat pump water heater, other measurements include the inlet and outlet water temperatures of the heat pump water heater and the volume of water leaving the heat pump water heater [10].

3.7. Plumbing system

The hot water leaving the heat pump water heater flows into a hot water supply manifold. The hot water supply manifold and a similar cold water manifold distribute water directly to each fixture, toilet, and water-utilizing appliance in the home through 1 cm cross-linked polyethylene (PEX) tubing. The entire length of tubing carrying hot water to each end-use is insulated. The dishwasher uses hot water, exclusively. The fixtures were manually adjusted to provide a mixed water temperature of approximately 41 °C at the sinks and showers, and 43 °C at the bathtubs [15]. Temperature measurements in conjunction with the accompanying flow rate data [10] are used to compute point of use temperatures.

3.8. Ventilation system

Outdoor air is supplied to the NZERTF via the heat recovery ventilator (HRV). This unit brings outdoor air into the house and continuously exhausts indoor air from the three bathrooms, with heat (but not moisture) exchange between the two airstreams to reduce the energy needed to condition the outdoor ventilation air. An HRV was selected in lieu of an energy recovery ventilator (ERV) in order to avoid reintroducing the moisture from the bathrooms into the house. The unit was sized to provide 137 m^3/h of outdoor air in accordance with the outdoor air requirements in ASHRAE Standard 62.2-2010 [16]. The actual outdoor airflow rate provided by the HRV has been measured on several occasions using a hot wire anemometer traverse and the results are approximately 171 m^3/h. This amount of indoor air was also continuously exhausted from the three bathrooms, which meets the requirement for continuous local bathroom exhaust in ASHRAE 62.2. This value, which exceeds the ASHRAE Standard 62.2 requirement by approximately 25%, resulted from selecting the lowest HRV fan speed (of the six possible) that exceeded the 137 m^3/h requirement. The effectiveness of the heat exchanger is determined using temperature measurements and periodic measurements of the HRV airflows [10]. The rated power consumption and effectiveness of the HRV are 54 W and 0.78, respectively.

The house has additional local air exhaust systems comprised of a kitchen exhaust fan and dryer exhaust. The kitchen exhaust fan is activated whenever the cooktop is energized, and the exhaust rate meets the minimum requirement for intermittent local kitchen exhaust in ASHRAE 62.2. When either of these appliances is on, a motorized damper in the attic is opened to permit, if needed, makeup air to enter the house through the attic. However, makeup

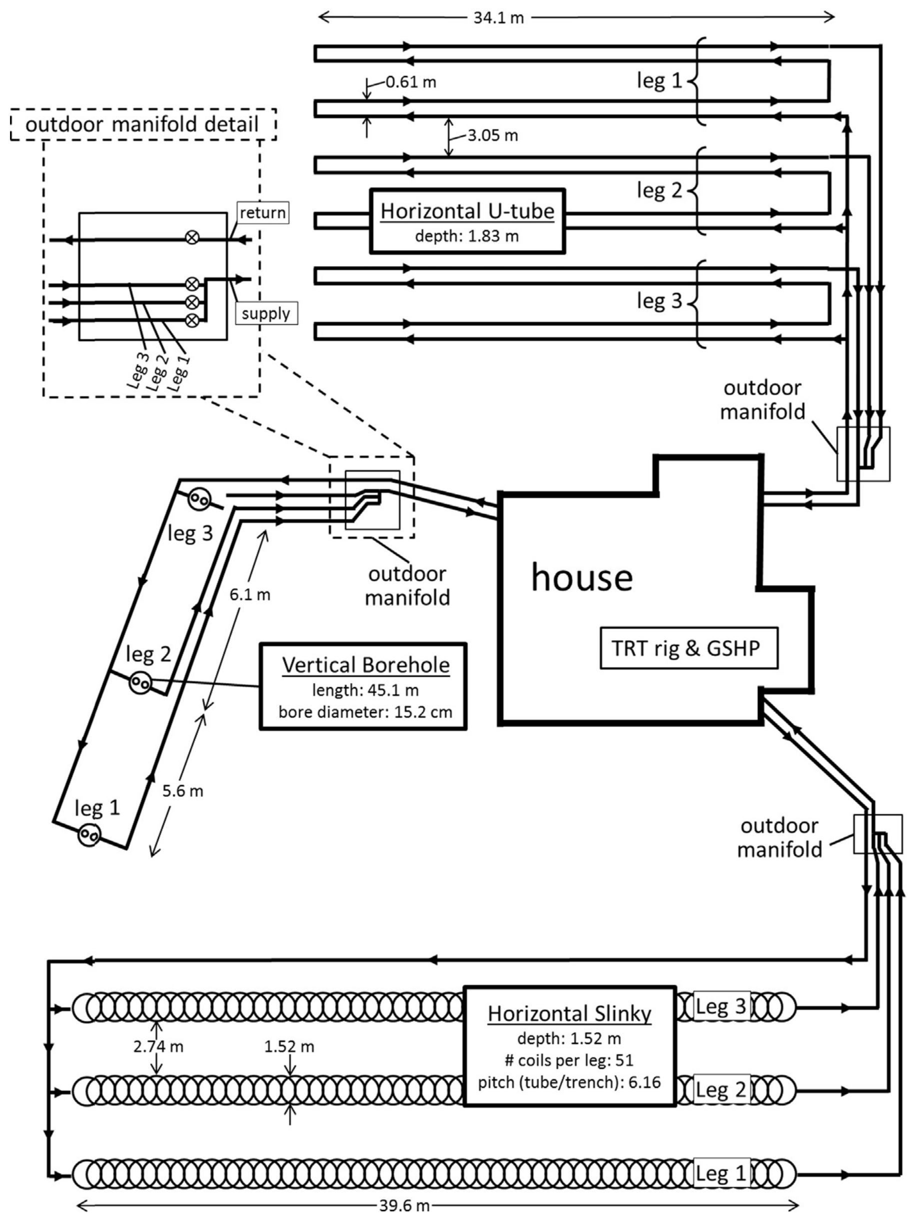

Fig. 6. Ground source heat exchangers.

air only enters the house when the indoor–outdoor pressure difference is greater than −10 Pa, controlled by means of a barometric damper downstream of the motorized damper.

3.9. *Systems for future research*

In addition to the previously described systems that were utilized during the first year of operation, the NZERTF contains a radiant floor heating system, ground-source heat exchangers, and a small duct high velocity air distribution system. A brief description of each system follows.

The basement slab of the NZERTF incorporates a 9-circuit radiant floor heating system for future research. The radiant floor tubing is placed 20.3 cm apart with a maximum circuit length of 76 m. The basement floor construction consists of a filter fabric laying on undisturbed soil, 10.2 cm of stone, 5.1 cm of extruded polystyrene insulation, a 0.15 mm polyethylene vapor barrier, and finally the 10.1 cm concrete slab with the embedded radiant floor tubing. The supply and return manifolds are accessible to permit the selection of individual or various combinations of the fluid circuits for future studies.

Three different sets of ground-source heat-exchangers (GSHX) were installed in close proximity to the NZERTF for future research: (1) vertical borehole (2) horizontal u-tube, and (3) horizontal slinky, Fig. 6. Each GSHX is independent and has been sized to meet the heating and cooling loads of the NZERTF when used in conjunction with an appropriately sized Ground Source Heat Pump (GSHP). The three GSHXs were instrumented [10] in order to permit future characterization of the heat transfer in the overall GSHX, each parallel leg within a given GSHX, local sections of main trench tubing, and supply/return tubing. A manifold inside the house allows researchers to select the appropriate GSHX. The tubing for all three heat exchangers consists of High Density Polyethylene (HDPE) black plastic. The nominal inside diameter of the tubing is 2.54 cm for the actual heat exchangers and 3.81 cm for the supply and return lines. Each of the three GSHX has three parallel legs that are joined together inside an outdoor manifold, Fig. 6.

Table 1
Miscellaneous electric plug loads and associated annual energy consumption.

Miscellaneous electric plug loads			
Loads	Annual energy (kW h)	Loads	Annual energy (kW h)
First color TV—simulated	127.3[a]	Laptop PC–simulated	72[b]
Second color TV—simulated	22.3[a]	Desktop PC–simulated	237[b]
DVD player—simulated	78[b]	PC monitor—simulated	85[b]
Video game system—simulated	41[b]	Printer (inkjet)—simulated	39
Clock radio—simulated	14.9	DSL/cable modem—simulated	17.6
Portable stereo—simulated	16.8	Hair dryer—actual	41.1
Rack stereo–simulated	153	Curling iron—simulated	1
Cable box–simulated	152.7	Vacuum cleaner—simulated	55[b]
Microwave—actual	135.1	Clock—simulated	26
Coffee maker (Drip)—simulated	61.2	Cordless phone—simulated	23.2
Toaster oven—actual	33.2	Cell phone charger—simulated	77.4
Toaster—actual	45.9	Answering machine—simulated	33.5
Blender—actual	7	Fan (portable)—simulated	11.3
Can opener—simulated	3	Heating pads—simulated	3
Hand mixer—actual	2	Iron—simulated	52.7
Slow cooker/crock pot—actual	16	Other	9.4
Wireless router—simulated	209.7[c]		

[a] The annual energy consumption for the First and Second color televisions are based on the occupancy profile. The First one is a 47 in. LED television and the Second one is a 32 in. LED television, and both are Energy Star rated.
[b] The annual energy consumption is obtained from Table 2.1.16 Operating Characteristics of Electric Appliances in the Residential Sector [4].
[c] The annual energy consumption is obtained by multiplying the estimated power (24 W) by number of hours in 52 weeks (8736 h).

The three vertical GSHX boreholes, separated by a nominal distance of 6.1 m, are 15.2 cm in diameter and extend 45.1 m below the depth of the supply/return tubing, which is 1.22 m beneath the surface of the earth. The tube separation spacing within the boreholes varies between 0 cm and 10.2 cm along the length of the bore. The tubes were grouted within the boreholes using bentonite clay grout, with a thermal conductivity of 0.73 W/m-°C. The horizontal u-tube GSHX trenches are 0.61 m wide, 34.1 m long and 1.8 m deep. Short-circuiting between the outgoing and returning tubes within a trench was minimized by carefully burying the tubes at the edges of the trench. The trenches were filled with soil and compacted every 0.3 m to ensure good soil-tube contact. The horizontal slinky GSHX trenches are 1.52 m wide, 39.6 m long and 1.52 m deep, with 2.74 m inter-trench spacing. Each trench leg has 51 coils of 1.52 m diameter and coil centers spaced every 0.76 m. The total length of coiled tubing in each leg is 244.2 m. The tube pitch, defined as the length of tube per length of trench, is 6.16. Similar to the horizontal u-tube GSHX, the slinky trench backfill was compacted every 0.3 m.

An air distribution system is in place that will permit the evaluation of high-velocity air distribution systems. The duct system consists of main trunk line that runs around the basement perimeter allowing takeoffs for individual rooms supply registers that provide air to the first floor. A supply riser feeds a similar perimeter run in the attic that serves rooms on the second floor. The trunk lines are 22.9 cm in diameter and designed for an air flow rate of 2039 $m^{3/}h$. The takeoff ducts that supply the individual registers are 5.1 cm in diameter.

4. Virtual family

The NZERTF utilizes a virtual family to emulate the energy and hot water consumption of a typical family. A virtual family offers the advantage of providing occupancy and energy use profiles that are repeatable, permitting future energy efficient technologies/energy saving strategies to be evaluated under identical energy use/occupant profiles. The number of occupants, occupancy profiles, water usage, and annual energy consumption of devices within the NZERTF were derived from the Building America Research Benchmark Definition [17].

4.1. Occupancy and lighting profiles

Four occupants are assumed to be living in the NZERTF. A minute-by-minute occupancy, lighting, and device usage schedule for each virtual family member is based upon a 7 day detailed narrative as presented in Omar and Bushby [18] and summarized by Kneifel [19]. Both parents were assumed to leave the house at 8:30 a.m. and return at 6:00 p.m. Both children leave the house at 8:00 a.m. with the eight-year old returning each day at 6:00 p.m., while the fourteen year old returns home at 6:00 p.m. on Mondays, Wednesdays, and Fridays and at 4:00 p.m. on Tuesdays and Thursdays. On weekends it was assumed that at least two members of the family are home at any given time. For simplicity and repeatability, the same weekly schedule is used the entire year. The lighting usage follows the occupancy profile of the family. No lights are energized when the family is sleeping at night or the house is unoccupied. Whenever a space is occupied by a virtual family member the lights in that space are energized.

4.2. Plug load profile

Simulating occupancy in the NZERTF requires operating various electric plug loads. Electric plug loads that would be found in at least 50% of all the households in the U.S. were incorporated into the NZERTF [1], Table 1. The strategy used to simulate plug loads (including cooking appliances) was to construct a schedule for each plug load such that over the course of the year the power required to operate the device times the hours of operation is equivalent to the annual energy consumption cited in Table 1. The plug load schedules are graphically presented by Kneifel [19] and discussed in detail by Omar and Bushby [18]. As noted in Table 1 some plug loads are actual appliances and others were simulated with resistive loads. Three separate techniques are used to control electrical loads: time-based, criteria-based, and cycle-based. The time-based plug loads are turned on and off by the DAS (or DAQ) at definitive times. The criteria-based plug loads are turned on by the acquisition/controller unit at a definitive time but de-energized when fixed criteria have been met. For example, the hair dryer is energized at a definitive time and is turned off by the data acquisition/controller unit when the energy consumed is equal to the

Table 2
Total daily moisture generated by cooking events and the NZERTF occupants.

Days	Moisture from cooking (L)	Moisture from people (L)	Total moisture (L)
Sunday	0.26	1.54	1.80
Monday	0.20	1.02	1.22
Tuesday	0.20	1.06	1.25
Wednesday	0.20	1.02	1.22
Thursday	0.20	1.06	1.25
Friday	0.20	1.02	1.22
Saturday	0.26	1.49	1.75

amount specified within the schedule. The cycle-based control is used for the clothes washer, clothes dryer, and dishwasher, where their loads are activated based on their start-times and allowed to complete their normal cycles. The number of cycles per week for the dishwasher, clothes washer, and the clothes dryer is based on a survey conducted by Proctor and Gamble and obtained from [20].

Cooking meals are simulated by an electric cooktop and an electric oven. The baseline annual energy use for smooth electric cooktops is 233.4 kW h, and for a self-cleaning electric oven is 303.7 kW h [21]. Each time the cooktop is used the range hood is also operated. The refrigerator is not subjected to the type of loads that would be present in a typical residence, such as opening doors or adding warm food. In order to compensate, an electrical resistor was placed inside the refrigerator and the power adjusted such that the annual energy consumption of the refrigerator is equivalent to that determined using the U.S. Department of Energy regulatory test method [22], 404 kW h. In addition, the automatic ice maker is operated continuously and its storage bin is emptied once per week.

4.3. Occupant sensible and latent loads

Simulating human occupancy requires accounting for the sensible and latent loads. In the NZERTF, sensible loads are simulated by resistors placed in the bedrooms, kitchen, and the living room areas operated in accordance with the occupancy schedule for each room. In order to introduce moisture into the NZERTF to represent the latent loads from cooking and the simulated human occupants, an ultrasonic humidifier is used [23].

To simulate latent load, the volume of moisture dissipated by the family through respiration-perspiration and cooking activities was determined. According to [24], the latent load per person, for seated and light work in an apartment, is 45 W. The value of latent heat of vaporization [25] was used to convert this value into a corresponding value of 0.07 L/h [18]. The latent load in [24] does not include the volume of moisture generated by cooking activities. Ref. [26] estimates that the moisture generated as a result of cooking breakfast, lunch, and dinner for a family of four is 0.17 L, 0.25 L, and 0.58 L, respectively. During the week, Monday through Friday, no one is home to prepare lunch so the moisture generated by cooking events only includes breakfast and dinner. The moisture generated on the weekends, however, includes all three meals. The daily moisture generated by the NZERTF family members account for the length of time that they are home, Table 2. The energy required to emulate the virtual family is not charged to the overall energy usage of the home since these electrical loads would not be normally present.

4.4. Occupant water consumption

The average daily water consumption for showers (123.7 L/day), baths (31.0 L/day), and sinks (110.3 L/day) for the virtual family was obtained from the average of three domestic hot water studies summarized in [17]. Thus the average total daily water usage is 265 L not including the water consumption by the dishwasher and the

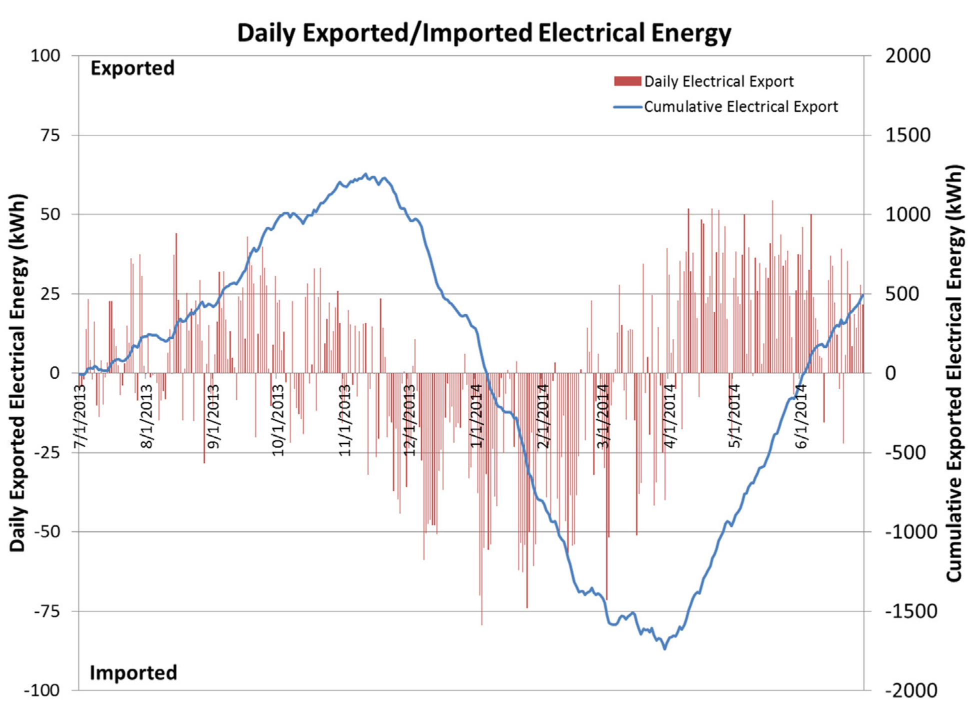

Fig. 7. Daily and cumulative net electricity usage.

Table 3
Monthly NZERTF thermal loads and energy consumption (kW h) by end use.

Month/Year	Jul/13	Aug/13	Sept/13	Oct/13	Nov/13	Dec/13	Jan/14	Feb/14	Mar/14	Apr/14	May/14	Jun/14	Annual
Heating load	0.0	0.0	0.0	56.4	830.4	1351.0	2156.9	1634.7	1423.5	252.7	0.0	0.0	7705.7
Cooling load	2122.9	1392.1	937.2	306.4	1.7	0.0	0.0	0.0	0.0	66.8	603.0	1559.7	6989.7
DHW load	252.4	217.8	238.2	268.5	283.2	325.9	343.1	330.0	340.5	300.3	276.9	250.6	3427.5
Heat pump heating	0.0	0.0	0.0	33.6	396.4	581.5	1254.8	753.1	650.4	113.2	0.0	0.0	3783.1
Heat pump cooling	700.8	481.0	345.4	142.3	15.7	0.0	0.0	0.0	0.0	13.6	177.7	511.3	2387.8
Heat pump water heater	53.3	70.8	57.0	82.5	129.8	156.3	142.8	125.0	120.7	72.7	55.2	46.1	1112.2
Solar system circulators	35.7	27.1	31.4	24.2	22.0	18.2	20.4	19.8	22.6	29.0	34.3	34.8	319.6
Lighting	37.5	31.9	36.1	37.8	36.3	36.6	36.9	32.9	36.2	38.1	39.5	35.6	435.4
Plug loads	202.5	167.1	199.7	210.2	208.5	210.2	214.0	193.8	216.7	206.3	208.2	202.5	2439.5
Heat recovery ventilator	42.4	35.6	42.3	44.4	43.7	44.3	46.4	38.7	45.3	42.8	45.4	43.1	514.4
Refrigerator	36.2	30.3	36.0	35.4	32.3	34.0	34.4	31.1	34.7	34.2	35.9	35.7	410.2
Dish washer	7.8	6.4	7.8	7.8	8.8	8.6	8.6	7.8	8.9	8.0	7.9	7.9	96.3
Cooktop	19.2	16.4	19.7	19.2	19.6	19.7	19.3	17.8	20.9	19.2	20.1	19.4	230.4
Oven	30.0	27.0	31.7	30.0	33.7	31.9	30.0	29.3	35.8	31.7	33.7	31.7	376.6
Clothes washer	5.2	4.6	6.2	6.2	6.1	6.3	6.2	5.6	6.4	6.0	6.1	6.0	70.8
Clothes dryer	47.6	39.8	45.9	44.8	46.8	46.9	45.7	41.2	50.8	44.1	44.2	44.0	541.8
Microwave	12.3	10.4	12.3	12.5	12.2	12.4	12.6	11.4	12.7	12.2	9.2	11.1	141.3
Total PV AC energy	1492.7	1162.4	1399.7	994.4	839.2	481.1	800.9	729.3	965.2	1425.1	1600.0	1633.3	13,523.4
Total energy consumed	1262.7	968.3	888.9	747.9	1025.0	1193.7	1891.4	1324.5	1269.4	689.2	733.7	1044.5	13,039.2
Net energy export	230.1	194.2	510.8	246.5	−185.8	−712.6	−1090.6	−595.3	−304.2	735.9	866.3	588.8	484.1

clothes washer. The water usage associated with the dishwasher and clothes washer is determined by their design/control features.

5. Results

A one-year demonstration period to demonstrate that the NZERTF could achieve net zero began July 1, 2013. The air-to-air heat pump system, previously described, was used to provide the space heating/cooling during the demonstration year. The earth-coupled heat exchangers, high-velocity air distribution system, and basement radiant floor heating system were not utilized. The house was operated as a single zone with constant thermostat set points of 23.8 °C and 21.1 °C during the cooling and heating seasons, respectively. Only two of the four solar thermal collectors in conjunction with the 303 L storage tank were utilized. The lights, appliances, plug loads, and sensible and latent loads associated with the virtual occupants were operated in accordance with the previously defined schedules. Selected results are presented in units of energy (kW h) and energy per unit area (kW h/m^2) of the conditioned space, 387 m^2, which includes the living area (252 m^2) and the basement (135 m^2).

Charcoal test kits were deployed to measure indoor radon concentrations in the house following the EPA Protocols for Radon and Radon Decay Product Measurements in Homes [27]. These measurements were made in the basement, first floor, and second floor. The average of all samples is below the EPA action level of 4 pCi/L [27]. The building materials for the NZERTF were specified to have low emissions of volatile organic compounds (VOC), including a prohibition on products with any added formaldehyde. Indoor air samples have been collected to measure the levels of approximately two dozen individual VOCs and formaldehyde in order to determine the impact of the building material specifications. These samples are collected monthly and will be used to determine if the VOC emission rates for the house change over time. Measurements to date [28] show that the use of medium density fiberboard and particleboard with no-added formaldehyde resins for cabinetry and other finished products effectively controlled the formaldehyde emissions and kept concentrations below levels in typical new homes. Monitoring of seasonal indoor VOC concentrations [28] suggests that building envelope components may be an overlooked source for some VOCs, especially aldehydes and alkanes.

Fig. 7 shows the daily and cumulative net electricity use for the first year of operation. A positive value indicates that the house produced more energy than it consumed and represents the quantity of energy exported to the grid. A negative value indicates that the house imported energy from the grid to meet the energy usage over the 24 h period. For the 12 months (July 2013 through June 2014) the house produced 484 kW h more electrical energy than it consumed, Table 3. The energy consumption by end use is tabulated in Table 3 and displayed graphically in the stacked bar chart, Fig. 8. The top five energy end uses for the twelve month interval are: (1) space conditioning (6685 kW h; 17.3 kW h/m^2), (2) plug loads (2440 kW h), (3) appliances (1868 kW h), (4) energy associated with producing hot water (sum of heat pump water heater and the solar thermal circulating pumps) (1432 kW h), and (5) lighting (435 kW h). The space conditioning energy consumption includes 514 kW h of energy consumed by the HRV. The energy usage by each individual appliance is shown in Fig. 9, with the clothes dryer consuming the greatest amount in this category.

The solar photovoltaic system and associated inverters experienced no malfunctions over the yearlong period converting 16.8% of the incident solar irradiance into AC electrical energy. As expected, the conversion efficiency of the photovoltaic array increases as the average cell temperature decreases, Table 4. The conversion efficiencies for December, January, February, and March were lower than expected as a result of the 8, 8, 12, and 10 days, respectively, when all or part of the solar array was covered with snow and/or ice for all or part of the daylight period. For all of the winter snow events, the reference cell plane of array irradiance detector cleared well in advance of the PV array. The monthly conversion efficiencies, from direct current to alternating current, of the photovoltaic system inverters all exceeded 94.5%.

The solar thermal hot water system provided 54% of the energy required to meet the domestic hot water load over the twelve month interval, Table 5. The solar thermal collectors were totally or partially covered with snow and/or ice during the same time intervals as the photovoltaic array. The two circulating pumps consumed 320 kW h during the year.

The solar hot water system malfunctioned for a total of 11 days in late August and early September as a result of an electrical fault in the glycol-circulating pump. The auxiliary heat pump water heater unit malfunctioned for 9 days in November and operated

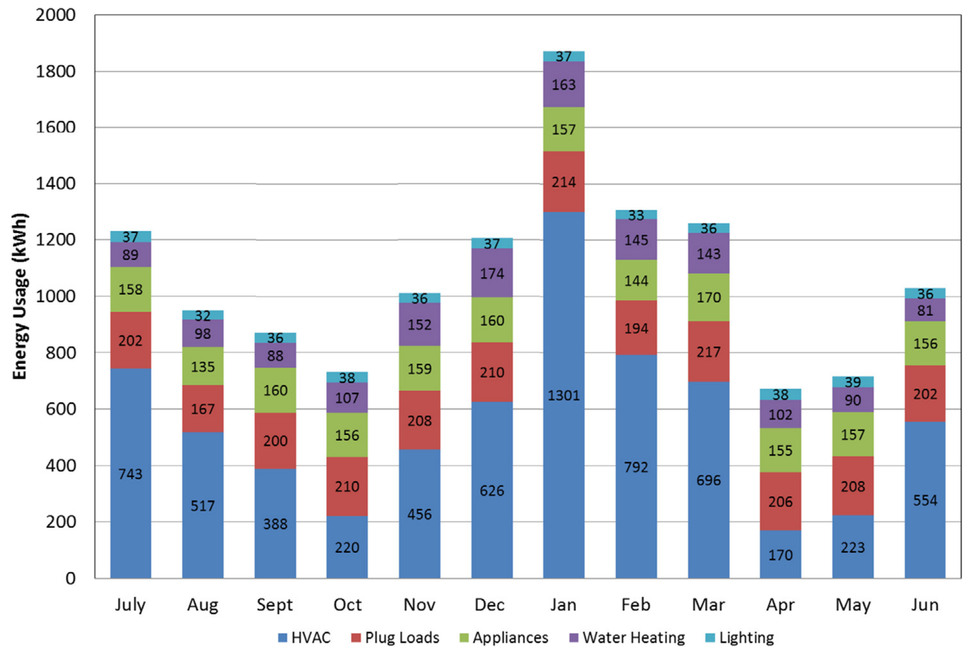

Fig. 8. Energy consumption by end use.

exclusively in the electric resistive mode as a result of a control wire becoming dislodged. Of the total energy consumed by the heat pump water heater unit, 975 kW h (88%) was consumed by the heat pump and controls and 137 kW h (12%) by the auxiliary resistive heating element.

Since testing commenced on July 1, 2013 the air-to-air heat pump system has performed without interruption. When operated in the cooling mode the unit operated with a seasonal COP (total thermal load/total electricity consumed) of 3.19 compared to the rated value of 3.82. There are two primary reasons that the measured seasonal cooling COP was less than the rated seasonal cooling COP. The seasonal cooling standby energy was 5.2% of the total heat pump energy consumed and is not taken into account in the rating procedure used to determine rated seasonal cooling COP. The second contributor is the fact that when the heat pump operated in the dedicated dehumidification mode, the COP is significantly less than when operating it its normal mode, Table 6. For example, in August 2013 the heat pump operated in the dedicated dehumidification mode approximately 41% of the time during which the measured COP was 0.89, Table 6. The current rating

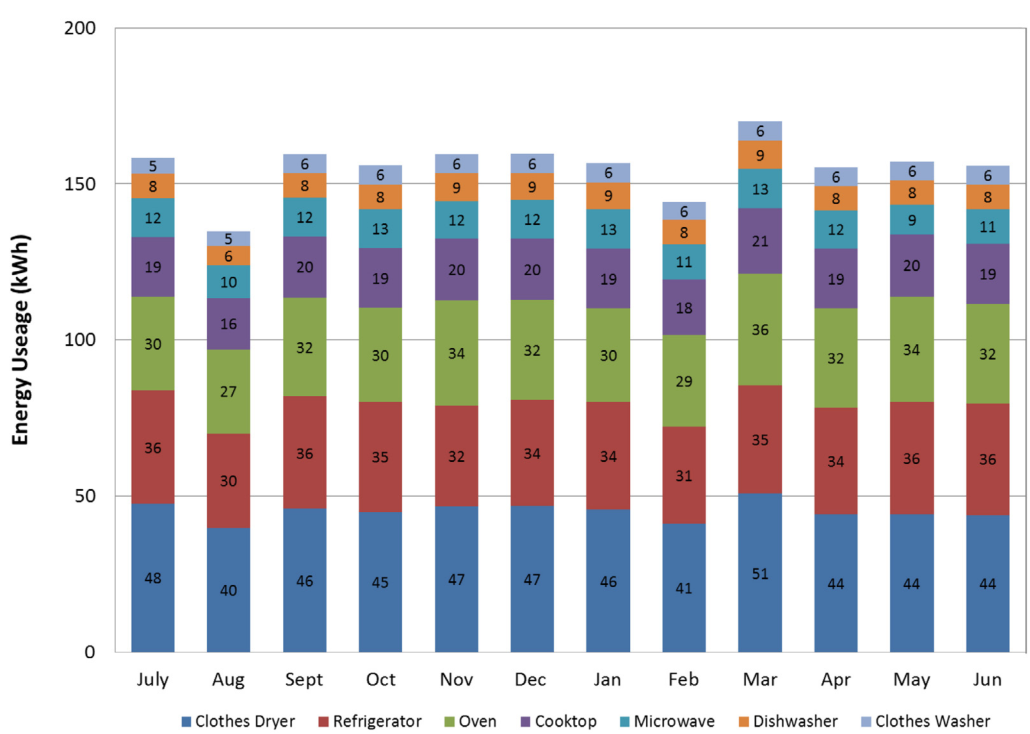

Fig. 9. Monthly energy consumption of appliances.

Table 4
Monthly photovoltaic system performance.

Month	Jul/13	Aug/13	Sep/13	Oct/13	Nov/13	Dec[a]/13	Jan[a]/14	Feb[a]/14	Mar[a]/14	Apr/14	May/14	Jun/14
Average daily incident solar energy on array[b] (kW h)	292.4	270.1	283.0	190.3	160.0	108.0	149.7	183.3	207.3	271.8	309.1	325.0
Average daily solar insolation on array[b] (kW h/m^2)	5604.0	5176.0	5424.0	3648.0	3067.0	2069.0	2868.0	3513.0	3972.0	5209.0	5924.0	6228.0
Average ambient temperature (C)	25.7	23.6	19.7	15.0	6.8	4.3	−1.9	1.1	4.1	12.7	18.7	23.6
Average cell temperature during energy generation (C)	38.6	36.7	35.1	26.5	15.9	11.1	7.2	10.8	15.1	24.2	32.8	37.6
Average daily delivered dc energy (kW h)	51.4	47.8	49.8	34.4	30.0	16.3	27.4	27.9	33.5	50.9	56.1	58.2
Array efficiency (%)	17.6	17.7	17.6	18.1	18.8	15.0	18.3	15.2	16.2	18.7	18.1	17.9
Average daily delivered AC energy (kW h)	49.3	45.7	47.7	32.8	28.6	15.4	26.0	26.7	31.9	48.6	53.7	55.7
Inverter efficiency (%)	95.9	95.6	95.8	95.5	95.3	94.5	95.1	95.4	95.2	95.6	95.7	95.7

[a] For 8 days in December, 8 days in January, 12 days in February, and 10 days in March the PV array was fully or partially covered with snow. If these days had been excluded the array efficiencies would have been 19.2%, 19.7%, 19.5%, and 19.2%, respectively, for December, January, February, and March.
[b] The Average Daily Incident Solar Energy on Array was determined using the framed area of an individual module (1.63 m^2) multiplied by the number of modules (32).

procedure does not address the degradation in performance that may occur when a heat pump unit operates in a dedicated dehumidification mode during a portion of the cooling season.

In the heating mode, the measured seasonal COP was 2.06 compared to the rated seasonal COP value of 2.65. The seasonal heating standby energy was 3.5% and is not considered in the rating procedure used to determine seasonal heating efficiency. The resistive heat is energized whenever the heat pump unit is in the defrost mode. The testing/rating procedure does not include the impact of resistive heat during the defrost cycle. Additionally, the resistance heat operated more frequently than anticipated, due to the inherent control logic of the thermostat. The thermostat heating configuration allows the user to prescribe a 1st stage differential, 2nd stage differential, 2nd stage delay time, and 3rd stage differential. The differential temperature is relative to the current set point temperature and the delay time is the maximum amount of time a given stage is allowed to operate before energizing the next higher stage. The cooling and heating mode differentials and delays, Table 7, were selected to maintain comfortable conditions throughout the year and minimize the use of resistive heat during the heating season. In the heating mode, 40 min was the maximum time the thermostat would permit the heat pump's compressor to operate in its high speed mode before energizing the electric resistance heat. This type of control logic appears to be effective in the cooling mode, but produced unnecessary usage of electric resistance heat in the heating mode. By limiting the high stage heat runtime to 40 min, the thermostat energized 3rd stage electric heat even though 2nd stage heating was increasing the temperature in the house and holding the indoor temperature within 0.6 °C of set point.

During the seven months that cooling was required in the NZERTF, the sensible to total load ratio varied from 0.58 to 0.78, Fig. 10. Currently most high efficiency heat pump systems operate with a sensible to total load ratio of greater than 80%. The higher latent loads associated with low energy homes will benefit from new technologies and control strategies that better address moisture removal. In the NZERTF enhanced moisture removal was made possible through the use of a heat pump that incorporated a dedicated dehumidification mode.

An analysis was performed to quantify the energy usage associated with the heat pump operation due to additional thermal loads introduced by the HRV. The HRV has two energy impacts, the fan energy and the increase or decrease in the thermal load resulting from introducing outdoor air into the house. For

Table 5
Monthly solar hot water and heat pump water heater system performance.

Month	Jul/13[a]	Aug/13	Sept/13[b]	Oct/13	Nov/13[c]	Dec/13[c]	Jan/14	Feb/14	Mar/14	Apr/14	May/14	Jun/14	Annual summary
Average outdoor temperature (°C)	25.7	23.6	19.7	15.1	6.8	4.4	−1.8	1.1	4.1	12.6	18.7	23.6	12.8
Average mains water temperature (°C)	22.9	22.8	23.0	21.1	18.8	16.8	15.4	14.5	14.9	16.0	18.8	20.7	18.8
Energy delivered to solar storage tank (kW h)	282.6	151.1	249.7	190.6	139.9	96.1	113.4	148.5	188.7	279.4	299.4	304.9	2444.4
Solar circulator pump energy consumption, E_{solar} (kW h)	35.7	27.1	31.4	24.2	22.0	18.2	20.4	19.8	22.6	29.0	34.3	34.8	319.6
Total energy used by heat pump water heater, E_{HP} (kW h)	53.3	70.8	57.0	82.5	129.8	156.3	142.8	125.0	120.7	72.7	55.2	46.1	1112.2
Energy used by heat pump water heater, resistive heat only (kW h)	0.0	5.8	3.2	3.2	44.3	36.1	13.9	14.2	12.8	3.3	0.6	0.0	137.4
Energy delivered by heat pump water heater tank, $Q_{del,HP}$ (kW h)	42.1	107.9	68.3	118.7	172.0	244.0	240.2	207.7	187.3	84.4	54.7	35.3	1562.6
Total hot water load, Q_{load} (kW h)	252.4	217.8	238.2	268.5	283.2	325.9	343.1	330.0	340.5	300.3	276.9	250.6	3427.5
Solar fraction, SF ()[d]	0.83	0.50	0.71	0.56	0.39	0.25	0.30	0.37	0.45	0.72	0.80	0.86	0.54
Solar energy factor, SEF ()	3.17	2.23	2.69	2.52	1.86	1.87	2.10	2.28	2.38	2.95	3.09	3.10	2.39

[a] Data loss on 7/1/2014 prevented calculation of Energy Delivered and Hot Water Load values for that day; therefore, SEF for July is computed for 7/2/2013–7/31/2013.
[b] Between 8/24/2013 and 9/3/2014, the pumps of the solar thermal water heater heat exchanger were not operational due to failure of electrical connection to glycol circulating pump.
[c] Between 11/25/2013 and 12/5/2013, the heat pump of the heat pump water heater was not operational due to a control wire being disconnected.
[d] $SF = 1 - (Q_{del,HP}/Q_{load})$; $SEF = Q_{load}/(E_{solar} + E_{HP})$.

Table 6
Monthly air-to-air heat pump system performance.

Month	Jul/13	Aug[a]/13	Sep/13	Oct/13	Nov/13	Dec/13	Jan/14	Feb/14	Mar/14	Apr/14	May/14	Jun/14
Thermal load[b]												
Heating mode (kW h)	0.0	0.0	0.0	56.4	832.1	1351.0	2156.9	1634.7	1423.5	252.7	0.0	0.0
Cooling mode (kW h)	2122.9	1392.1	937.2	306.4	1.7	0.0	0.0	0.0	0.0	66.8	603.0	1559.7
Heat pump energy usage												
Heating mode (kW h)	0.0	0.0	0.0	33.6	396.4	581.5	1254.8	753.1	650.4	113.2	0.0	0.0
Cooling mode (kW h)	700.8	481.0	345.5	142.3	15.7	0.0	0.0	0.0	0.0	13.6	177.7	511.3
Resistive heat (kW h)	0.0	0.0	0.0	13.6	103.0	117.0	547.6	196.4	169.4	10.2	0.0	0.0
Avg. outdoor temp (°C)	26.6	24.6	20.7	15.5	7.1	4.5	−1.5	1.0	4.1	13.1	19.7	24.5
Avg. indoor temp (°C)	23.6	23.5	23.5	22.4	21.0	21.0	20.9	20.9	21.0	21.2	22.9	23.3
Degree heating days	0.0	0.0	30.7	218.8	610.0	773.5	1107.3	873.3	792.6	301.0	45.9	0
Degree cooling days	924.9	682.5	580.5	325.0	61.4	39.1	0.0	0.0	22.8	196.3	542.1	785.4
Heating run time (h)	0.0	0.0 .2	0.0	14.9	181.5	314.1	460.9	370.7	305.1	10.2	0.0	0.0
Cooling run time[c] (h)	492.1		256.3	81.2	17.5	0.0	0.0	0.0	0.0	52.6	133.8	395.6
Dehumidification mode (h)	164.9	143.8	70.0	38.0	17.5	0.1	0.0	0.0	0.0	0.0	13.8	133.2
Dehumidification (L/kW h)	1.35	1.30	1.20	1.10	0.29	0.70	–	–	–	–	1.04	1.23
Coefficient of performance												
Heating mode (–)	0.00	0.00	0.00	1.68	2.10	2.32	1.72	2.17	2.19	2.23	0.00	0.00
Cooling mode (–)	3.03	2.89	2.71	2.15	0.11	0.00	0.00	0.00	0.00	4.90	3.39	3.05
COP1 (dehumidification)[d]	0.93	0.89	0.91	0.76	0.20	0.48	–	–	–	–	0.71	0.84

[a] Missing data Aug 2 through Aug 6, 2013.
[b] Heat pump thermal load includes electric resistance heat.
[c] Cooling run time includes the time the unit operated in the dehumidification mode.
[d] Dehumidification COP equals the average of the daily dehumidification COP values (total latent energy divided by electrical energy during active dehumidification).

Table 7
Air-to-air heat pump thermostat settings.

Mode	1st Stage differential (°C)	2nd Stage differential (°C)	2nd Stage delay time (min)	3rd Stage differential	3rd Stage delay time
Cool	1.1	2.8	40	NA	NA
Heat	0.56	1.1	10	3.3 °C	40 min

example, when the outdoor air temperature is lower than the indoor air temperature additional energy will be required to heat the home during the heating season compared to an identical home without a fresh air ventilation system. During the cooling season, the introduction of outdoor air may increase or decrease the sensible and latent loads, dependent on the outdoor air temperature and moisture content relative to the indoor temperature and relative humidity. The use of the HRV can also be compared to the hypothetical situation of meeting the ventilation requirement using a balanced ventilation system without a HRV to introduce

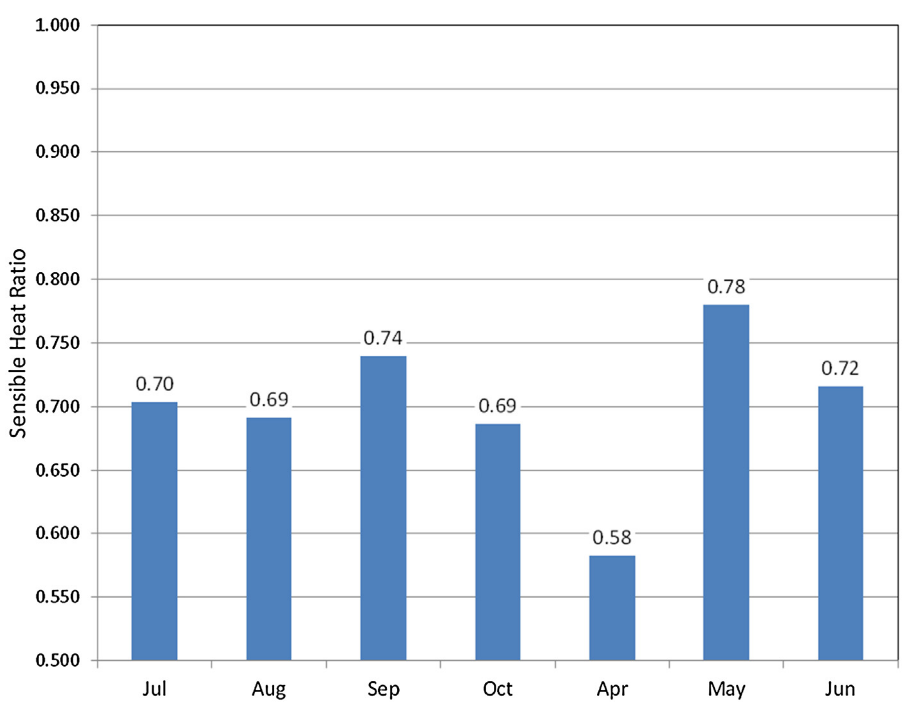

Fig. 10. Monthly sensible heat ratio during cooling months.

Table 8
Monthly heat recovery ventilator performance.

Month/Year	Jul/13	Aug/13[a]	Sept/13	Oct/13	Nov/13	Dec/13	Jan/14	Feb/14	Mar/14	Apr/14	May/14	Jun/14
Energy consumption (kW h)	42.4	35.6	42.3	44.4	43.7	44.3	46.4	38.7	45.3	42.8	45.4	43.1
Average ambient temperature (°C)	26	24	20	15	7	4	−2	1	4	13	19	24
Average outdoor air temp. to HRV (°C)	26	24	20	16	8	6	1	4	6	13	19	24
Average indoor temp. to HRV (°C)	24	24	24	22	21	21	21	21	21	21	23	24
Average HRV exhaust temperature (°C)	26	24	22	18	13	12	9	11	12	16	21	24
HRV effectiveness (–)	0.62	0.61	0.71	0.75	0.76	0.74	0.73	0.74	0.75	0.75	0.75	0.74
Average flow rate (m^3/h)	174	192	180	194	186	206	208	205	207	195	201	193
Sensible load[b] introduced by HRV(kW h)	−18.7	4.9	54.4	106.8	204.5	244.5	314.3	245.4	243.5	122.0	62.2	4.8
Latent load[c] introduced by HRV (kW h)	511.7	282.9	40.1	−23.5	−138.4	−106.0	−106.8	−70.7	−58.2	−76.0	−23.4	233.1
Additional heat pump electrical energy used to meet HRV ventilation load (kW h)[d]	229.6	191.6	−5.4	−30.7	32.1	154.9	417.1	201.1	189.5	−16.9	−77.0	165.0
Sensible load introduced by balanced ventilation system, no HRV (kW h)	−81.1	−10.1	122.5	236.2	491.0	591.9	763.0	593.6	591.3	293.0	133.4	−21.1
Latent load introduced by balanced ventilation system, no HRV (kW h)	513.6	290.4	62.3	12.3	−113.1	−80.4	−80.1	−52.7	−38.1	−54.3	3.7	262.1
Additional heat pump electrical energy used to meet balanced ventilation system (No HRV) load (kW h)[e]	201.7	167.2	−15.6	1.7	58.6	198.6	538.5	229.1	232.3	29.9	−64.5	154.1
Difference in heat pump energy–no HRV vs HRV ventilation relative to HRV ventilation (%)	−4.0	−5.0	−1.8	18.4	6.4	7.5	9.6	3.8	6.6	35.9	7.0	−2.1

[a] Missing data for Aug-2 through Aug-6, 2013.

[b] Sensible loads are the sum for the month with positive sensible indicating cooling and negative indicating heating the house. Some days the HRV or the mechanical ventilation system helped the cooling or heating system and some days the HRV or mechanical system worked against the heating or cooling system.

[c] Latent loads should be equal but differ due to using living room relative humidity and temperature for the exhaust air when doing calculations for mechanical ventilation. HRV calculations where done with living room relative humidity and the temperature measured at the HRV for the exhaust air. A negative latent load occurred when moisture was removed from the house.

[d] Heat pump electrical is the reduction or increase in the energy consumed by the heat pump as the result of introducing fresh air utilizing the HRV.

[e] Heat pump electrical is the reduction or increase in the energy consumed by the heat pump as the result of introducing the same quantity of fresh air as the HRV case but with no heat recovery.

the same quantity of outdoor air. During the one-year period, the HRV consumed a total of 514 kW h in fan energy, Table 3. It is assumed the fan power required for the balanced ventilation system without an HRV would be equivalent to the ventilation system utilizing a HRV. Table 8 captures the energy impact of the HRV and ventilating to the same degree using a balanced ventilation system without a HRV. When space cooling was required, the use of the HRV resulted in an increase of 187 kW h (0.5 kW h/m^2) and 1048 kW h (2.7 kW h/m^2) in the sensible and latent loads, respectively, over the 12 month test interval. Using a balanced ventilation system (no HRV) that introduces the same quantity of outdoor air, the sensible and latent cooling loads would have been increased by 316 kW h (0.8 kW h/m^2) and 1168 kW h (3.0 kW h/m^2), respectively. When space heating was required the HRV increased the sensible load by 1402 kW h (3.6 kW h/m^2) and decreased the latent load by 583 kW h (1.5 kW h/m^2). Using a simple balanced ventilation system without a HRV when space heating was required would have increased the sensible load 3387 kW h (8.8 kW h/m^2) and reduced the sensible load 442 kW h (1.1 kW h/m^2).

Table 8 shows that use of an HRV increased the electrical energy consumption of the heat pump more than would have been the case if a balanced ventilation system without an HRV had been used for the months of July-2013, August-2013, September-2013 and June-2014. In those months the use of a balanced ventilation system without a HRV would have reduced the electrical energy used by the heat pump system (Table 3) by 4.0%, 5.0%, 1.8%, and 2.1%, respectively compared to the measured heat pump consumption using the HRV. During the months of October-2013, November-2013, December-2013, January-2014, February-2014, March-2014, April-2014 and May-2014, use of the HRV decreased the heat pump electrical energy consumption compared to the energy that would have been consumed if a balanced mechanical ventilation system without a HRV had been used with the difference ranging from 3.8% to 35.9%, Table 8. For the cooling months, when the reduction in the sensible load was greater than if a balanced ventilation system without a HRV had been used the total electrical consumption of the heat pump is greater due to the fact that the latent loads are larger and the heat pump has a significantly lower COP when operated in the dehumidification mode as compared to the normal mode. The annual energy required to ventilate the house using the HRV is the total of the additional energy to run the heat pump, 1451 kW h (3.7 kW h/m^2), to meet the additional thermal load introduced by the HRV, plus 514 kW h of HRV fan energy, for a total of 1965 kW h (5.1 kW h/m^2). If a balanced mechanical ventilation system without an HRV had been used the total annual energy consumed would have been 1732 kW h (4.5 kW h/m^2) of additional heat pump energy to meet the load introduced by the balanced ventilation system (without an HRV) plus 514 kW h of assumed fan energy or 2246 kW h (5.8 kW h/m^2). This finding is climate dependent. In this case, the HRV would result in less energy consumption during the heating months and more energy during the cooling months compared to a balanced ventilation system without a heat recovery ventilator.

6. Lessons learned

In addition to quantitative data presented in this paper, a number of lessons were learned during the design and operation of the NZERTF. Using a well designed and implemented building envelope, efficient building energy technologies, and appropriately sized solar photovoltaic and thermal systems, it was possible to achieve net-zero for a house with conventional architecture, amenities, and size comparable to those being constructed in the surrounding area. The living area of the NZERTF (252 m^2) is comparable to the average size home (242 m^2) currently being constructed in the United States.

The photovoltaic and thermal solar systems were significantly impacted by snow cover during the demonstration period. For 38 of the 365 days the photovoltaic and thermal panels were totally or partially covered by snow. The photovoltaic system, consisting of four parallel strings of eight modules connected in series, is significantly impacted by snow cover when any given module(s) within a string is snow covered as a shaded photovoltaic module can current limit the entire string. Significant periods of time for the snow cover on the photovoltaic panels to melt were observed as a result of the well-insulated roof assembly keeping heat loss to a minimum.

The actual performance of a heat pump system can be expected to be less than its rated performance. The rated performance, based upon laboratory tests, does not include the standby energy that is consumed when the unit is not providing space conditioning. Additionally, whenever the NZERTF heat pump entered into the defrost mode the controls energized a backup resistive heater. The test procedure does not capture the energy impact of the resistive heat during defrost cycles. During the cooling season the heat pump unit operated in the dedicated dehumidification mode for significant portions of time. The test procedure/rating procedure does not reflect the reduced performance of the heat pump when it operates in the dehumidification mode. During the time intervals that the heat pump unit is operating in the dehumidification mode the COP is significantly lower, Table 6. Finally, the manner in which the thermostat operates the heat pump, previously discussed, can have a significant impact on the heat pump's performance that is not reflected by laboratory testing/test procedures used to rate heat pumps.

7. Conclusions

A net-zero energy residential test facility has been constructed on the campus of the National Institute of Standards and Technology in Gaithersburg, MD. The facility has demonstrated that a residence similar in size, aesthetics, and features to those in the surrounding communities can achieve net-zero energy operation. During the first year of operation the residence generated 13,523 kW h of electricity using the 10.2 kW solar photovoltaic system. The house consumed 13,039 kW h (33.7 kW h/m^2) energy while meeting the electrical and comfort needs of a typical four member family, resulting in a net energy export of 484 kW h.

The solar photovoltaic system converted 16.8% of the incident solar radiation into useful electrical energy. The solar thermal hot water system provided 54% of the energy required to meet the domestic hot water load. The greatest end use of electricity within the residence was for space conditioning, followed by plug loads, and appliances. Ventilating the house to exceed the ASHRAE Standard 62.2-2010 requirement using an HRV resulted in 1965 kW h (5.1 kW h/m^2) of energy consumption: 514 kW h to power the HRV fan and an additional 1451 kW h (3.7 kW h/m^2) of energy being used by the heat pump to meet the additional sensible and latent loads. This represents 31.8% of the energy consumed by the heat pump, 15.0% of the total energy consumed by the house, and 14.5% of the energy generated by the photovoltaic system. If the HRV had provided the exact flow rate specified by ASHRAE Standard 62.2-2010 requirement, 137 m^3/h versus the measured flow rate of 171 m^3/h, and assuming identical fan power in both cases, it is estimated that the total energy impact of the HRV would have been 1676 kW h (4.3 kW h/m^2) or 12.8% of the house's total annual energy consumption.

The NZERTF has a vast array of features and capabilities that will be utilized in the future. Over 200 future research and development opportunities suggested by 22 organizations are summarized in Domich et al. [29]. Recommended "research and development opportunities" within this document range from practical tests for assessing the airtightness of building enclosures to dynamic control of the heating, cooling, and ventilation systems taking full advantage of emerging "smart grid" capabilities.

Among the lessons learned during this one year study was significant impact that snow and/or ice can have on the output of a photovoltaic system attached to an extremely well-insulated roof. Significant periods of time were needed for the snow/ice cover to melt as a result of the well-insulated roof assembly. It was also observed that a simple control device, such as the heat pump's thermostat, can have a significant impact on the energy needed during the heating season. Despite these challenges, it was shown that net-zero can be achieved for a home slightly larger than the average size currently being constructed in the U.S. with all the amenities and features of a modern home.

References

[1] United States Department of Energy, Buildings Energy Data Book: 2011. Available at ⟨http://buildingsdatabook.eren.doe.gov/default.aspx⟩ (last accessed 12.02.14).

[2] D.S. Parker, Very low energy homes in the United States: perspectives on performance from measured data, Energy Build. 41 (5) (2009) 512–520.

[3] E. Musall, T. Weiss, K. Voss, A. Lenoir, M. Donn, S. Cory, F. Garde, Net zero energy solar buildings: an overview and analysis on worldwide building projects, international energy agency solar heating & cooling Task40/ECBCS Annex52, in: Conference Proceedings Eurosun, 2010.

[4] S. Rosta, R. Hurt, R. Boehm, M.J. Hale, Performance of a zero-energy house, J. Sol. Energy Eng. 130 (2008) 021006–21011.

[5] D.R. Boleyn, Reaching toward "Net Zero": results from a PVT powered residence in the Pacific Northwest, Conf. Proc. Sol. Conf. 6 (2012) 4203–4209.

[6] M.D. Doiron, W. O'Brien, A. Athienitis, Energy performance, comfort, and lessons learned from a near net zero energy solar house, Conf. Proc. ASHRAE 117 (2) (2011) 585–596.

[7] J. Sherwin, C. Colon, D. Parker, E. Martin, Performance of four near zero energy homes: lessons learned, Proceedings of the ASHRAE Thermal Performance of the Exterior Envelopes of Whole Buildings XI International Conference, December 5–9 (2010) 5–9.

[8] P. Norton, C. Christensen, E. Hancock, G. Barker, P. Reeves, The NREL/habitat for humanity zero energy home: a cold climate case study for affordable zero energy homes, National Renewable Energy Laboratory, in: Technical Report, NREL/TP-550-43188, 2008.

[9] ASHRAE Inc., Chapter 25—thermal and water vapor transmission data-2009, in: ASHRAE Handbook of Fundamentals, ASHRAE Inc., Atlanta, GA, 2009.

[10] M.W. Davis, W.M. Healy, M. Boyd, W.V. Payne, H. Skye, L. Ni g, T. Ullah, Monitoring techniques for the net-zero energy residential test facility, in: NIST Technical Note 1854, 2014.

[11] AHRI, Standard for performance rating of unitary air-conditioning and air-source heat pump equipment, Air-Conditioning, Heating, and Refrigeration Institute, 2111 Wilson Boulevard, Suite 500, in: AHRI 2008. Standard 210/240, AHRI, Arlington, VA, 2008 (22201).

[12] International Electrotechnical Commission (IEC), Crystalline silicon terrestrial photovoltaic (PV) modules—design qualification and type approval, in: IEC Standard 61215, International Electrotechnical Commission (IEC), Geneva, Switzerland, 2005.

[13] W. Bower, C. Whitaker, W. Erdman, M. Behnke, M. Fitzgerald, Performance Test Protocol for Evaluating Inverters Used in Grid-Connected Photovoltaic Systems, 2004.

[14] SRCC™ Standard 100, in: Test Methods and Minimum Standards for Certifying Solar Collectors, Solar Rating & Certification Corporation, Cocoa, FL, 2012.

[15] ASHRAE, Table 3 representative hot-water temperatures, chapter 50: service water heating, in: 2011 ASHRAE Handbook—HVAC Applications, ASHRAE, Inc., Atlanta, GA, 2011.

[16] ASHRAE, ANSI/ASHRAE Standard 62.2-2010: Ventilation for Acceptable Indoor Air Quality, American Society of Heating, Refrigerating and Air-Conditioning Engineers, Inc., Atlanta, GA, 2010.

[17] R. Hendrom, in: Building America Research Benchmark Definition, Technical Report No. NREL/TR 550-44816, National Renewable Energy Laboratory, Golden, CO, 2008.

[18] F. Omar, S.T. Bushby, Simulating occupancy in the NIST net-zero energy residential test facility, in: NIST Technical Note 1817, 2013.

[19] J.D. Kneifel, Annual whole building energy simulation of the NIST net-zero energy residential test facility, in: NIST Technical Note 1767, 2012.

[20] C. Iglehart, N. Milesi-Ferretti, M. Galler, Consumer use of dishwashers, clothes washers, and dryers: data needs and availability, in: NIST Technical Note 1696, 2011.

[21] Technical Support Document for Residential Cooking Products, Volume 2: Potential Impact of Alternative Efficiency Labels for Residential Cooking Products, Lawrence Berkeley National Laboratory, Berkeley, CA, 1998.

[22] U.S. Department of Energy's Regulatory Test Method, 10CFR430, Sub part B, Appendix A, 47 FR 34526, 2011.

[23] X. Fang, D. Christensen, G. Barker, E. Hancock, Field Test Protocol: Standard Internal Load Generation for Unoccupied Test Homes, Building Technologies Program, U.S. Department of Energy, 2011.

[24] ASHRAE, Table 1, Chapter 18: nonresidential cooling and heating load calculations, in: 2013 ASHRAE Handbook—Fundamentals, 2013.

[25] J.L. Monteith, Latent heat of vaporization in thermal physiology, Nat.: New Biol. 236 (64) (1972) 96.

[26] R. Barnhart, Home Moisture, Minnesota Department of Commerce, Minnesota, 2012.

[27] EPA, Protocols for Radon and Radon Decay Product Measurements in Homes, U.S. Environmental Protection Agency, Washington, DC, 1993.

[28] D. Poppendieck, L. Ng, M. Schlegel, A. Persily, A. Hodgson, Long Term Air Quality Monitoring in a Net-Zero Energy Residential Test Facility Designed with Specifications for Low Emitting Interior Products, Indoor Air, Hong Kong, China, 2014.

[29] P.D. Domich, B. Pettit, A.H. Fanney, W.M. Healy, Research and development opportunities for the NIST net-zero energy residential test facility, in: NIST Technical Note 1869, 2015.